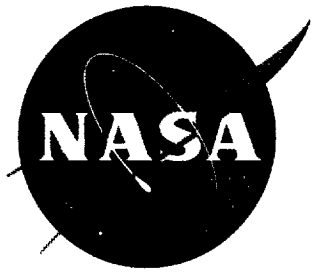

TECHNICAL MEMORANDUM

X-713

COMPARISON OF FULL-SCALE LIFT AND DRAG CHARACTERISTICS OF THE X-15 AIRPLANE WITH WIND-TUNNEL RESULTS AND THEORY

By

Edward J. Hopkins
Ames Research Center
Moffett Field, Calif.

and

David E. Fetterman, Jr.
Langley Research Center
Langley Field, Virginia

and

Edwin J. Saltzman
Flight Research Center
Edwards, Calif.

NATIONAL AERONAUTICS AN
WASHINGTON

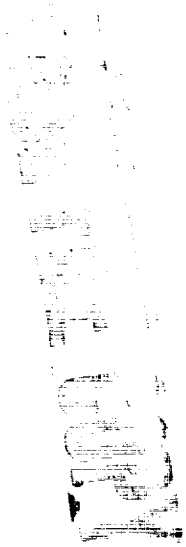

1G

[redacted]

NATIONAL AERONAUTICS AND SPACE ADMINISTRATION

TECHNICAL MEMORANDUM X-713

COMPARISON OF FULL-SCALE LIFT AND DRAG CHARACTERISTICS OF THE X-15 AIRPL[redacted]WITH WIND-TUNNEL RESULTS AND THEORY* **

By Edward J. Hopkins, David E. Fetterman, Jr., and Edwin J. Saltzman

SUMMARY

A comparison is made between the minimum drag of the X-15 as measured in flight and the minimum drag of an X-15 wind-tunnel model extrapolated to flight Reynolds numbers. In addition, the trimmed lift and drag-due-to-lift characteristics, obtained from wind-tunnel model tests, are shown to be in agreement with full-scale results for Mach numbers up to about 5. Existing theoretical methods are indicated to be adequate for estimating the X-15 minimum drag but underestimated the drag due to lift and overestimated the maximum lift-drag ratio. Two-dimensional theory is shown to be adequate for predicting the base pressures behind surfaces having very blunt trailing edges, such as those on the vertical tail of the X-15.

Author

INTRODUCTION

Recent X-15 flights up to a Mach number of 6 permit comparisons to be made between flight and wind-tunnel results and existing supersonic and hypersonic theories throughout a Mach number range not heretofore covered. For aircraft having surfaces with extremely blunt trailing edges, such as the X-15, the base drag represents a very large portion of the minimum drag. Therefore, the base drag measured in flight on the various components of the X-15 airplane, including the vertical fins, the side fairings, and the fuselage, will be compared with the base drag measured on a wind-tunnel model. The adequacy of two-dimensional theory for predicting the base pressures behind surfaces having very blunt trailing edges is also shown.

---

*This document is based on a paper presented at the Conference on the Progress of the X-15 Project, Edwards Air Force Base, Calif., November 20-21, 1961.

**Title, Unclassified.

[redacted]

[redacted]

SYMBOLS

C_D	drag coefficient
C_{D_B}	base-drag coefficient
$\frac{dC_D}{dC_L^2}$	average slope of the drag-due-to-lift factor measured between $C_L = 0$ and C_L for maximum lift-drag ratio
$\Delta C_{D_{SB}}$	speed-brake drag-coefficient increment
C_L	lift coefficient
C_{p_B}	base-pressure coefficient
L/D	lift-drag ratio
M	free-stream Mach number
p_B	base pressure
R	Reynolds number based on free-stream conditions and body length (49.83 ft, full scale)
T'	reference temperature
T_w	wall temperature
T_{ad}	adiabatic wall temperature
α	angle of attack, deg
δ_h	horizontal-tail deflection, deg

Subscripts:

max	maximum
min	minimum

H
2
7
4

[redacted]

DISCUSSION

The lift and drag flight data presented herein were obtained during power-off gliding flights in which gradual push-down, pull-up maneuvers were performed. Examination of the flight records indicated that negligible or zero pitching acceleration was encountered during this flight maneuver. Accelerometers were used to determine the lift and the total drag. A more detailed description of the method for obtaining flight drag data is given in reference 1. The flight data to be presented herein include some of the data of reference 2, which were limited to Mach numbers below 3.1, and data obtained in recent flights. Full-scale flight drag measurements should be conducted under prescribed conditions which are best suited for the particular airplane and instrumentation system. Such conditions did not exist for some of the maneuvers included in this paper. For this reason, the X-15 flight drag results cannot be considered final until data from such prescribed maneuvers have been obtained.

H 2 7 4

Typical drag characteristics obtained during power-off flight at Mach numbers of 3 and 5 are shown in figure 1. For some of the flight results to be presented, it was necessary to extrapolate the drag curves to obtain values of the minimum drag, since the lift coverage was insufficient to define the entire drag curve.

Except for the minimum drag coefficient, the trimmed lift and drag characteristics for the wind-tunnel models were derived from reference 3 and unpublished data on a 0.020-scale model tested in the Langley Unitary Plan wind tunnel at a Mach number of 4.65. Wind-tunnel data from reference 4 were used for Mach numbers of 2.29 and 2.98; however, for the trim characteristics as applied herein the center-of-gravity position is believed to be at 20-percent mean aerodynamic chord rather than at 16-percent mean aerodynamic chord as quoted in the reference. This alteration of the center-of-gravity position is supported by comparisons between the pitching-moment data of reference 4 and the aforementioned tests on the 0.020-scale model in the same facility at a Mach number of 4.65, and also on recent tests of a 0.067-scale model in the Ames Unitary Plan wind tunnel at a Mach number of 3.0. These comparisons indicated that better agreement between the various tests occurs when the center-of-gravity position for the data of reference 4 is assumed to be located at 20-percent mean aerodynamic chord.

Increments of drag for the speed brake were taken from references 4 and 5. The recent tests conducted in the 8- by 7-foot test section of the Ames Unitary Plan wind tunnel included measurements of the minimum drag of the 0.067-scale model of the X-15 airplane with the boundary layer tripped by distributed roughness particles placed a constant distance from the leading edge of all wing and tail surfaces. The

[redacted]

distance selected for fixing transition was 5 percent of the average chord of the exposed wing surface, since this distance corresponded approximately to the average length of laminar flow as measured in flight at a Mach number of 3. The boundary layer was also tripped on the fuselage and the side fairings at this same distance. The drag of the roughness particles was evaluated from separate measurements of the drag of the model with particles of several different sizes and was subtracted from the total drag. This model was also equipped with the nose boom and all other protuberances, including the camera fairings, antennas, retracted landing skids, pitot probe, and exhaust vents found on the flight airplane. Base pressures were measured on the side fairing, the fuselage, and the upper and lower vertical fins to facilitate comparisons between the experimental and theoretical values of the minimum drag with the base drag removed. The minimum drag is compared on this basis since no known methods are available to account for the interference effects from the wakes of the blunt surfaces on the base drag.

H 2 7 4

In order to make a valid comparison between wind-tunnel and flight results, it is necessary to adjust the skin-friction drag, which is included in the wind-tunnel data, to values corresponding to flight Reynolds numbers. The results for extrapolating[1] the minimum drag as measured in the wind tunnel by the T' method of references 6 and 7 to flight Reynolds numbers at Mach numbers of 2.5 and 3 are shown in figure 2. For this extrapolation, the recovery temperature was assumed to be that for an adiabatic smooth flat plate having a turbulent boundary layer and a recovery factor of 0.88. At flight Reynolds number for the Mach number of 3, the increment of drag calculated to account for the difference between the skin-friction drag of an adiabatic flat plate and that for a flat plate having the minimum temperature measured on the rearward portion of the fuselage is also shown. A more exact skin-friction correction to the extrapolated minimum drag for an adiabatic flat plate at flight Reynolds number should, of course, take into account the different temperatures which would exist on each of the components of the X-15. However, because of the relatively small skin-friction increment shown, which represents a temperature differential of 438° F $\left(T_{ad} = 538° \text{ F}, \quad (T_w)_{min} = 100° \text{ F}\right)$, the effect of these different component temperatures does not appear to be too significant at Mach numbers of 3 and below. At Mach numbers above 3, however, this increment of skin friction would become larger, because of the greater difference between the adiabatic wall temperature and the actual temperatures of

[1]In the extrapolations to flight conditions shown herein, it was assumed that the wave-drag coefficient did not vary with Reynolds number. This assumption was confirmed by calculations which indicated that boundary-layer-displacement effects were negligible on the X-15 configuration at Mach numbers of 3 and below.

the X-15 surfaces. For the Mach numbers shown, the T' method appears to give a satisfactory extrapolation of the minimum drag from wind tunnel to flight for the Reynolds numbers considered here. In figure 2 the flight data have a small increment of drag subtracted because the airplane did not have zero horizontal-tail deflection for zero lift coefficient. No such adjustment was made to any other data to be presented.

The effect of Mach number on the minimum drag with the base drag removed is shown in figure 3. In calculating the skin-friction drag by the T' method at the higher Mach numbers and corresponding Reynolds numbers, the skin temperature was considered to be the maximum which would be calculated for the central portion of the wing during a prescribed (not actual) flight maneuver. The effect of heat transfer and radiation on the surface temperature was considered. These maximum calculated temperatures, together with the flight conditions corresponding to the flight data presented in figure 3, are:

M	R	$T_{w_{max}}$, °R
1.1	82×10^6	448
1.4	115	511
1.5	115	534
1.9	80	635
1.9	63	655
2.1	62	705
2.3	118	785
2.5	62	835
2.6	95	866
3.0	57	994
3.3	58	1,109
4.0	70	1,267
4.3	22	1,357
5.0	19	1,597
5.0	12	1,662
6.0	33	1,649

The wave drag of the surfaces and the fuselage for the supersonic theory was computed on an electronic computing machine by the method of Holdaway and Mersman given in reference 8. This method is based on the theory of reference 9. The wave drag of the protuberances such as the camera fairings, retracted skids, standard NASA airspeed boom, hypersonic flow-direction sensor when used, and antennas was estimated separately from reference 10 and is included in the wave-drag increments shown.[2] For

[2]In general, the X-15 was equipped with the standard NASA airspeed boom at a Mach number of 3 and below and with the hypersonic-flow-direction sensor at higher Mach numbers.

hypersonic theory, the wave drag of the fuselage, the hypersonic-flow-direction sensor, the blunt leading edges, and the protuberances was calculated from Newtonian theory (for example, ref. 11). At the lowest Mach numbers, the sum of the skin friction and the wave drag from supersonic theory shows good agreement with the flight points, but at the higher Mach numbers this theory underpredicted the flight data. Hypersonic theory shows general agreement with the flight data between Mach numbers of 4 and 6.

The average value of the trimmed drag due to lift as measured at low lift coefficients is presented for power-off flight as a function of Mach number in figure 4. For the wind-tunnel and theoretical values of the drag due to lift, the center of gravity was assumed to be located at its average position for flight, 22 percent of the mean aerodynamic chord. For both the supersonic and hypersonic theories, the mutual interference factors for the wing-body and the tail-body combinations were estimated from reference 12. The lift-curve slopes for the wing and tail alone were calculated by linear theories given in references 13 and 14 for the supersonic theory. For hypersonic theory, the lift of these components was calculated from the shock-expansion theory for two-dimensional flat plates with a correction applied for the three dimensionality of the flow from the charts in reference 15. The effect of the expansion flow field from the wing on the tail lift was accounted for in the hypersonic theory by the method described in reference 16. Since the negative dihedral placed a large portion of the horizontal tail below the wing vortex field, no interference effects from the wing vortices on the tail lift were considered for either theory. In both theories the drag due to lift was considered to be equal to the product of the lift of the surface and the sine of the flow angle relative to the surface; thus, no leading-edge thrust was assumed. Up to a Mach number of about 5, the wind-tunnel data show excellent agreement with the flight data. This result is representative up to an angle of attack for $(L/D)_{max}$, since insufficient flight data were available at the higher attitudes. Both theories, however, underestimate the flight drag due to lift throughout the Mach number range.

Some insight into the factors that contribute to these low theoretical estimates can be gained from figure 5, which shows the trimmed lift and horizontal-tail deflection as a function of angle of attack at a Mach number of about 5 for power-off flight. The wind-tunnel data show general agreement with flight data. Both theories give good predictions of trimmed lift coefficient but considerably underestimate the tail deflections for trim; hence the theoretical estimates of the drag due to lift are low (see fig. 4). The difficulty of predicting the tail inputs is believed to be due primarily to the effect of the gap between the horizontal tail and the side fairing, which progressively increases with tail deflection, and also to the complex flow field existing behind the wing. In the theories no gap effects were considered.

However, as noted previously in the hypersonic theory, downwash and local dynamic-pressure variations on the horizontal tail were determined from considerations of the shock-expansion field behind the wing.

The trimmed maximum lift-drag ratio is shown as a function of Mach number in figure 6. The theoretical curves are based on the estimated values of wave drag, friction drag, and drag due to lift previously discussed. In addition, the base drag, which must be included, was assumed to be the same as that measured in power-off flight. The wind-tunnel data show excellent agreement with the flight values. The theories, however, overestimated the flight $(L/D)_{max}$, primarily because of the underestimated drag due to lift.

H 2 7 4

In the foregoing comparisons either the base drag was removed from the total drag, or the base drag measured in power-off flight was assumed. The various components of the base drag are now considered. It should be noted that all of the full-scale base-drag or base-pressure-coefficient data which follow (figs. 7 to 10) are for the XLR99 engine installation. However, for some of the preceding figures there are flight data, at $M \leq 3$, representing the LR11 or interim-rocket-engine installation. Where this is the case, base drag from the LR11 installation applies.

The base-drag coefficients measured on the vertical fins, the side fairings, and the fuselage are shown as a function of Mach number both for power-on and power-off flight conditions in figure 7. In each sketch the shaded regions are the areas being considered. It can be seen that engine operation significantly affected the pressures on the fuselage and the vertical fins but had a much smaller effect on the pressures for the side fairing. The wind-tunnel data are somewhat below the power-off flight results, probably because of the influence of the sting support.

Ratios of base drag to minimum drag as measured on each of the base components in power-off flight are shown in figure 8. It can be seen that the vertical fin is the largest contributor to the base drag, contributing even more than the fuselage. Note that the total base drag decreases from about 60 percent of the total minimum drag at a Mach number of about 1.5 to about 17 percent at a Mach number of 5.2.

The average base pressure measured in power-off flight on the upper vertical fin is shown as a function of Mach number in figure 9. The theoretical curve for the two-dimensional theory of Korst (ref. 17) has been verified by past wind-tunnel tests on relatively thin wings with blunt trailing edges. It is noteworthy that base-pressure characteristics for surfaces as blunt as the vertical fin of the X-15 (ratio of chord to thickness of 5.5) were also adequately predicted by two-dimensional theory. At Mach numbers above 4, the flight

[redacted]

base-pressure coefficients approach the limiting curve ($p_B = 0$). At Mach numbers above 5, the hypersonic approximation of base-pressure coefficient $\left(-1/M^2\right)$ gives reasonable agreement with the flight results.

The base pressures measured on the fuselage and the side fairing are compared in figure 10 with values from the two-dimensional theory of Korst and with values for a body of revolution (without fins) according to Love (ref. 18). It can be seen that the two-dimensional theory, particularly at Mach numbers between about 2 and 3, gives a better estimate of the flight base pressures than Love's curve. The fact that the fuselage base pressures agree better with the two-dimensional theory than with Love's curve is probably associated with the wake interference from the blunt vertical fins and the side fairings.

The increment of drag produced by deflecting the speed brakes 35° is shown as a function of Mach number in figure 11. The increments of drag measured in the wind tunnels show general agreement with those measured in flight. Between Mach numbers from about 3 to 5, Newtonian theory gives a good estimate of this drag increment. It can be seen that the increment of drag from the speed brakes approximately equals the minimum drag at the low Mach numbers and is about 35 percent greater at a Mach number of 5.5.

CONCLUDING REMARKS

For Mach numbers up to about 5 and in the low angle-of-attack range, wind-tunnel trimmed lift and drag due to lift obtained on models showed excellent agreement with flight results on the X-15. Furthermore, at least up to a Mach number of 3 and for the Reynolds number range considered herein, flight data indicate that reasonable values of the full-scale minimum drag can be obtained from extrapolations of wind-tunnel results to flight Reynolds numbers, provided that the condition of the boundary layer is known and that a representative wind-tunnel model is tested, even to the extent of including all the protuberances found on the full-scale airplane. Existing theoretical methods were adequate for estimating the X-15 minimum drag; these theories, however, underestimated the drag due to lift and overestimated the maximum lift-drag ratio. This result was due primarily to the inability of the theories to predict the control-surface deflections for trim. It was also shown that two-dimensional theory, which has been known to predict the base pressures on relatively thin wings with blunt trailing edges,

[redacted]

also predicts satisfactorily the base pressures behind the extremely blunt vertical surface of the X-15.

Flight Research Center
National Aeronautics and Space Administration
Edwards, Calif., November 20, 1961

H
2
7
4

[redacted]

[redacted]

REFERENCES

1. Beeler, De E., Bellman, Donald R., and Saltzman, Edwin J.: Flight Techniques for Determining Airplane Drag at High Mach Numbers. NACA TN 3821, 1956.

2. Saltzman, Edwin J.: Preliminary Full-Scale Power-Off Drag of the X-15 Airplane for Mach Numbers From 0.7 to 3.1. NASA TM X-430, 1960.

3. Penland, Jim A., and Fetterman, David E.: Static Longitudinal, Directional, and Lateral Stability and Control Data at a Mach Number of 6.83 of the Final Configuration of the X-15 Research Airplane. NASA TM X-236, 1960.

4. Franklin, Arthur E., and Lust, Robert M.: Investigation of the Aerodynamic Characteristics of a 0.067-Scale Model of the X-15 Airplane (Configuration 3) at Mach Numbers of 2.29, 2.98, and 4.65. NASA TM X-38, 1959.

5. Leupold, Mathias J., and Freeman, Elizabeth M.: A Second Series of Supersonic Force Tests on the Full-Span Model X-15 for North American Aviation, Inc. Rep. 200, Naval Supersonic Lab., M.I.T., Sept. 1958.

6. Sommer, Simon C., and Short, Barbara J.: Free-Flight Measurements of Turbulent-Boundary-Layer Skin Friction in the Presence of Severe Aerodynamic Heating at Mach Numbers From 2.8 to 7.0. NACA TN 3391, 1955.

7. Bertram, Mitchel H.: Calculations of Compressible Average Turbulent Skin Friction. NASA TR R-123, 1962.

8. Holdaway, George H., and Mersman, William A.: Application of Tchebichef Form of Harmonic Analysis to the Calculation of Zero-Lift Wave Drag of Wing-Body-Tail Combinations. NACA RM A55J28, 1956.

9. Jones, Robert T.: Theory of Wing-Body Drag at Supersonic Speeds. NACA Rep. 1284, 1956. (Supersedes NACA RM A53H18a.)

10. Hoerner, Sighard F.: Fluid-Dynamic Drag. Publ. by the author (148 Busteed Drive, Midland Park, N.J.), 1958.

11. Grimminger, G., Williams, E. P., and Young, G. B. W.: Lift on Inclined Bodies of Revolution in Hypersonic Flow. Jour. Aero. Sci., vol. 17, no. 11, Nov. 1950, pp. 675-690.

[redacted]

12. Pitts, William C., Nielsen, Jack N., and Kaattari, George E.: Lift and Center of Pressure of Wing-Body-Tail Combinations at Subsonic, Transonic, and Supersonic Speeds. NACA Rep. 1307, 1957.

13. Lapin, Ellis: Charts for the Computation of Lift and Drag of Finite Wings at Supersonic Speeds. Rep. No. SM-13480, Douglas Aircraft Company, Inc., Oct. 14, 1949.

14. Eichelbrenner, E. A.: Portance Des Ailes En Fleche Aux Vitesses Supersoniques. La Recherche Aéronautique (O.N.E.R.A.), No. 25, Jan.-Feb. 1952, pp. 19-20.

15. Harmon, Sidney M., and Jeffreys, Isabella: Theoretical Lift and Damping in Roll of Thin Wings With Arbitrary Sweep and Taper at Supersonic Speeds - Supersonic Leading and Trailing Edges. NACA TN 2114, 1950.

16. Dugan, Duane W.: Estimation of Static Longitudinal Stability of Aircraft Configurations at High Mach Numbers and at Angles of Attack Between 0° and ±180°. NASA MEMO 1-17-59A, 1959.

17. Korst, H. H.: A Theory for Base Pressures in Transonic and Supersonic Flow. Jour. Appl. Mech., vol. 23, no. 4, Dec. 1956, pp. 593-600.

18. Love, Eugene S.: Base Pressure at Supersonic Speeds on Two-Dimensional Airfoils and on Bodies of Revolution With and Without Fins Having Turbulent Boundary Layers. NASA TN 3819, 1957. (Supersedes RM L53C02.)

[redacted]

[redacted]

FLIGHT DATA
POWER OFF

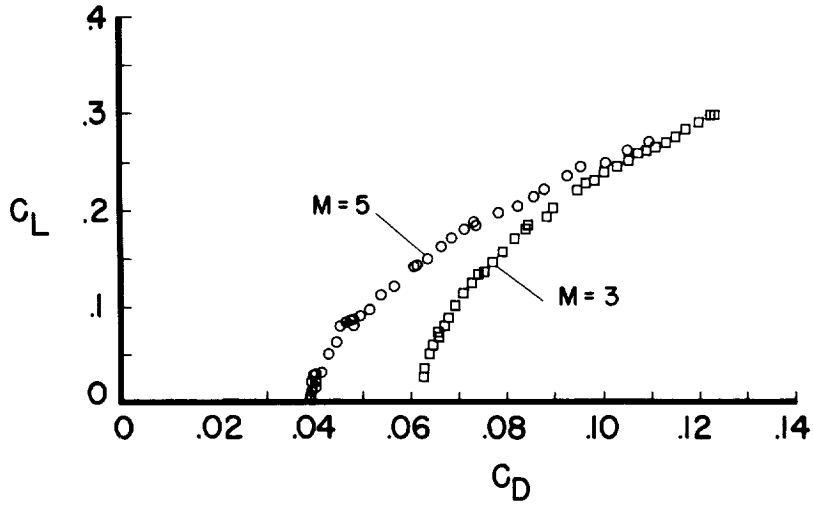

Figure 1

EFFECT OF REYNOLDS NUMBER ON
MINIMUM DRAG

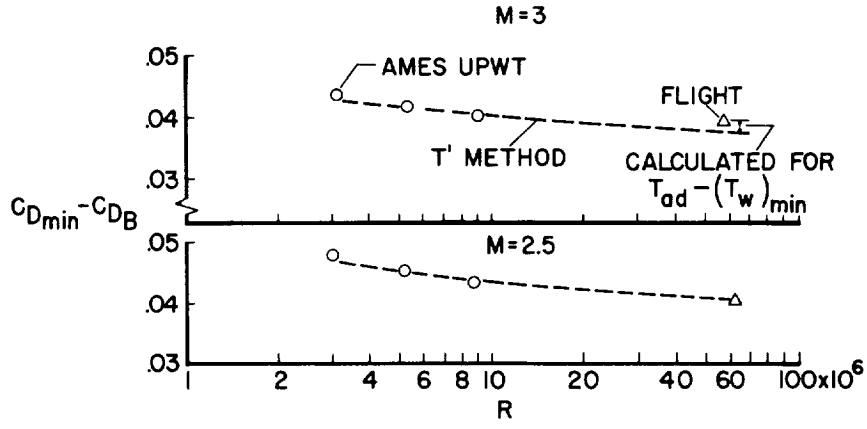

Figure 2

[redacted]

EFFECT OF MACH NUMBER ON MINIMUM DRAG
POWER OFF

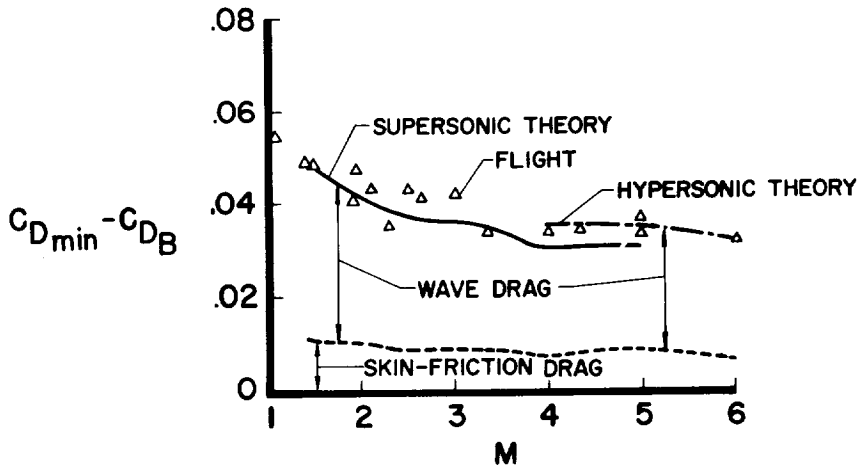

Figure 3

EFFECT OF MACH NUMBER ON THE TRIMMED DRAG DUE TO LIFT
POWER OFF

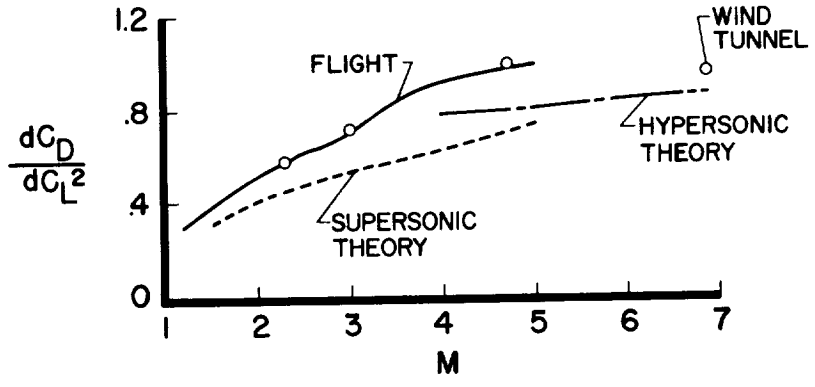

Figure 4

[redacted]

TRIMMED LIFT AND HORIZONTAL-TAIL DEFLECTIONS
POWER OFF
M=5

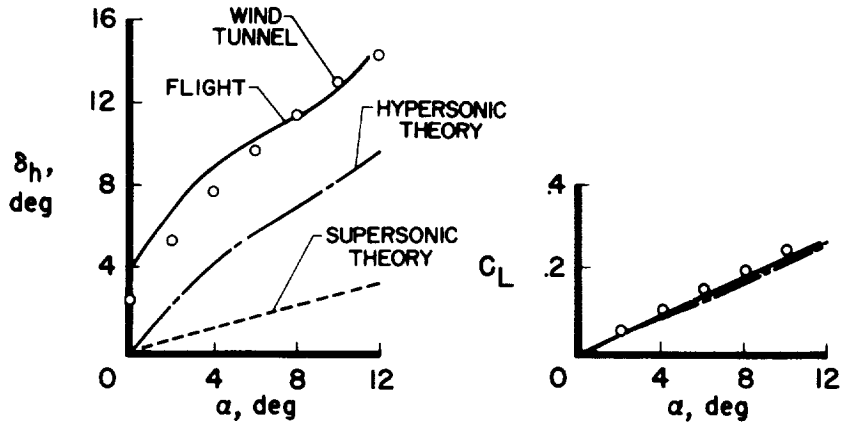

Figure 5

EFFECT OF MACH NUMBER ON THE TRIMMED MAXIMUM LIFT-TO-DRAG RATIO
POWER OFF

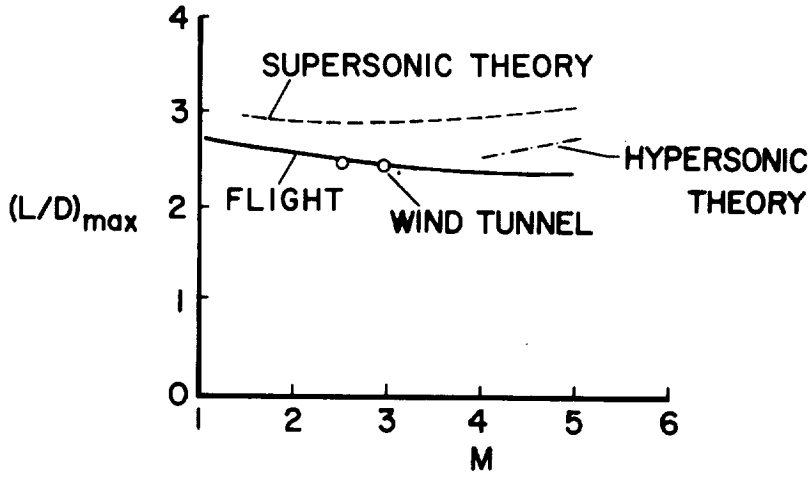

Figure 6

[redacted]

BASE-DRAG VARIATION WITH MACH NUMBER

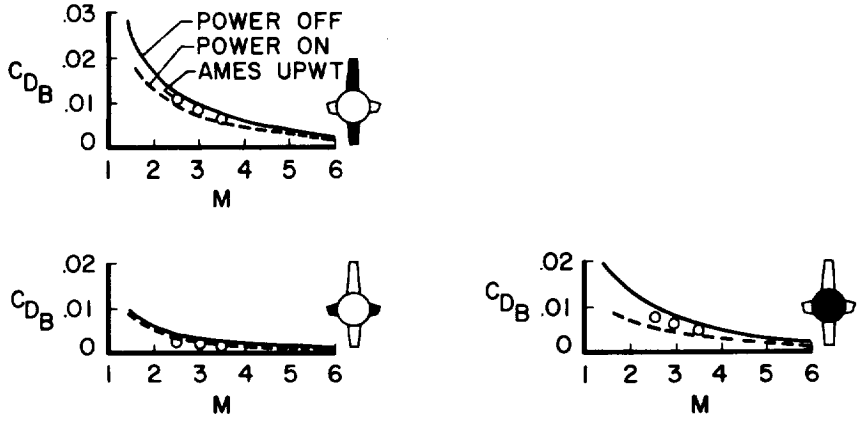

Figure 7

EFFECT OF MACH NUMBER ON RATIO OF BASE DRAG TO MINIMUM DRAG

POWER OFF FLIGHT

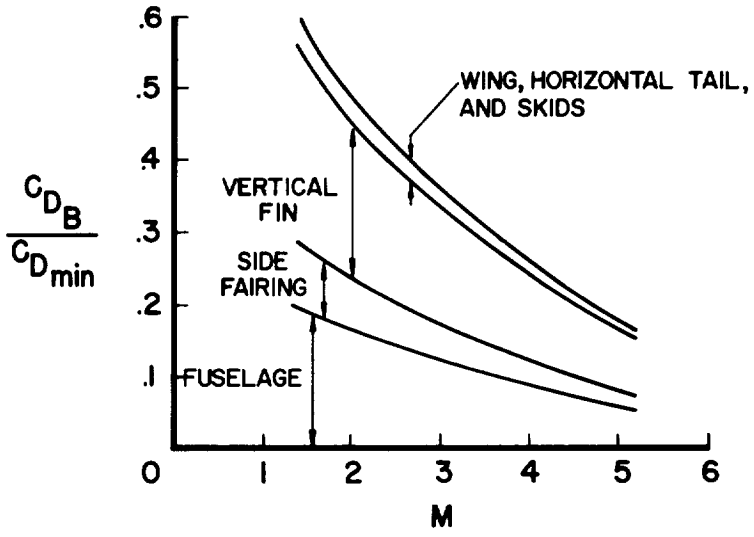

Figure 8

[redacted]

BASE PRESSURES FOR UPPER VERTICAL FIN

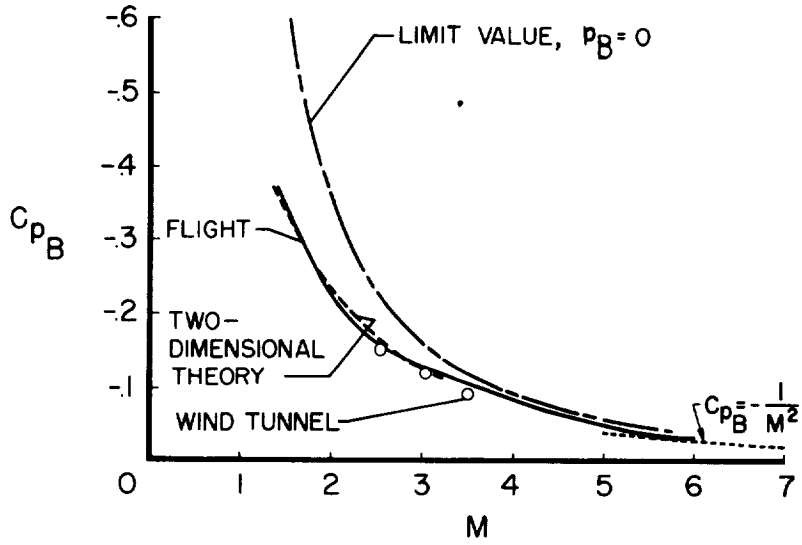

Figure 9

FUSELAGE AND SIDE-FAIRING BASE-PRESSURE COEFFICIENTS

POWER OFF

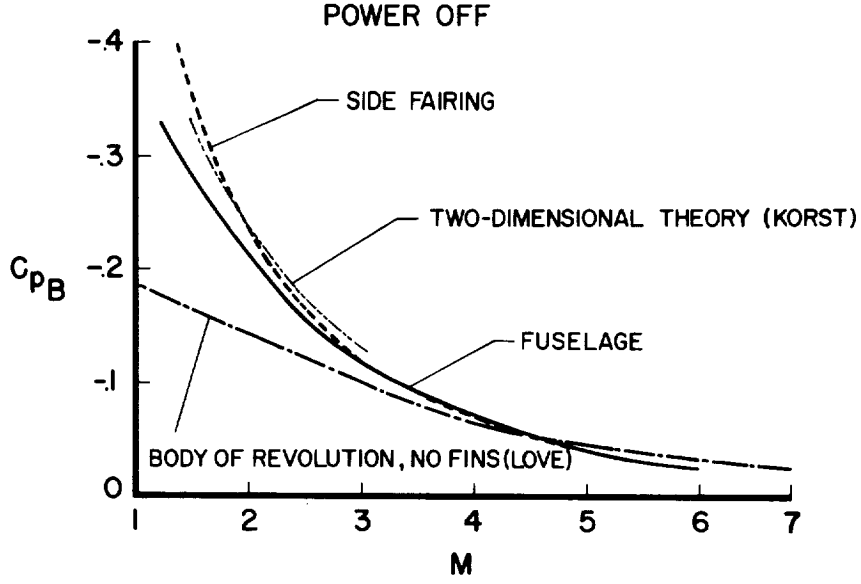

Figure 10

[redacted]

[redacted]

SPEED-BRAKE DRAG INCREMENT

POWER OFF

$\Delta C_{D_{SB}} = C_{D_{SB\ OPEN}} - C_{D_{SB\ CLOSED}}$

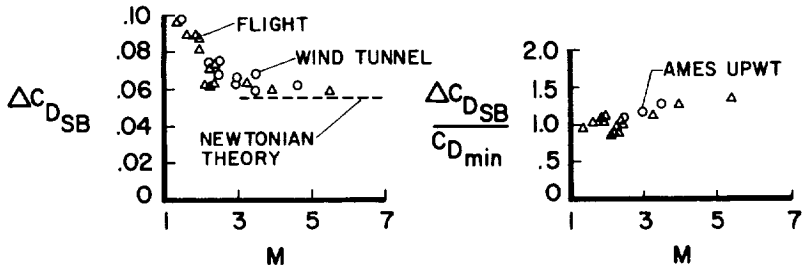

Figure 11

[redacted]

[redacted]

[redacted]